Uryga-Bugajska, I, Borman, DJ, Pourkashanian, M, Catalanotti, E and Wilson, C (2011) *Theoretical investigation of the performance of alternative aviation fuels in an aero-engine combustion chamber.* Proceedings of the Institution of Mechanical Engineers, Part G: Journal of Aerospace Engineering. (In Press)

XML Template (2011)
K:/application/sage/Plg/PIG 402277.3d

[15.4.2011–12:21pm]
(PIG)

[1–12]
[PREPRINTER stage]

1

Theoretical investigation of the performance of alternative aviation fuels in an aero-engine combustion chamber

I Uryga-Bugajska[1]*, **M Pourkashanian**[1], **D Borman**[1], **E Catalanotti**[1], and **C W Wilson**[2]

[1]School of Process, Environmental and Materials Engineering, CFD Centre, The University of Leeds, Leeds, LS2 9JT, UK

[2]Department of Mechanical Engineering, The University of Sheffield, Sheffield, S1 3JD, UK

Abstract: When considering alternative fuels for aviation, factors such as the overall efficiency of the combustion process and the levels of emissions emitted to the atmosphere need to be critically evaluated. The physical and chemical properties of a fuel influence the combustion efficiency and emissions and therefore need to be considered. The energy content of a biofuel, which is influenced negatively by the presence of oxygen in the molecular structure (i.e. oxygenated chemical compounds), is relatively low when compared with that of conventional jet fuel. This means that the overall efficiency of the process will be different. In this article, two possible scenarios have been investigated in order to assess the potential to directly replace conventional jet fuel – kerosene with methyl buthanoate – MB (a short chain fatty acid methyl ester – representing biofuel) and a synthetic jet fuel (Fischer–Tropsch fuel) using computational fluid dynamics (CFD) modelling in a typical modern air-spray combustor. A detailed comparison of kerosene with alternative fuel performance has been made. In addition, the impact of fuel blending on the combustion performance has been investigated. The CFD results indicate that there are notable differences in the engine performance and emissions when replacing conventional jet fuel with alternative fuels. The effect of alternative fuel chemistry on the combustion characteristics is noticeable both in the flamelet calculation and the CFD main flow field computations. This is particularly the case for MB.

Keywords: CFD modelling, aircraft engine, combustion, alternative aviation fuel, biofuel, FT fuel, methyl butanoate, FAMEs

1   INTRODUCTION

Petroleum products have always been considered as supreme fuels for the transportation sector due to their beneficial combination of high energy content, performance, availability, and ease of handling at a low cost. However, the continuing increases in oil price, concern over energy security, and the reducing availability of petroleum have focused the industry into investigating alternative fuel solutions. In the aviation industry, there is a strong focus on developing bio-aviation and other alternative fuels that can be used with current engine technology [1]. Although commercial aircraft are only responsible for around 3 per cent of total emissions compared with other sectors, the impact of emissions being directly into the upper atmosphere means that they potentially have a more pronounced effect on changes in the climate [2, 3]. Utilizing alternative fuels in aviation is a challenge, but there is the potential to reduce the quantities of engine emissions released into the atmosphere from aircraft. One of the most important issues is the challenge to find a suitable candidate to

Corresponding author: School of Process, Environmental and Materials Engineering, CFD Centre, The University of Leeds, Leeds, LS2 9JT, UK.

email: pmiu@leeds.ac.uk

supplement or even replace conventional kerosene. A number of possible directions are considered and presented in this article.

The main objective of this study has been to investigate the effect of using alternative aviation fuel, specifically biofuel (MB) and synthetic fuel (*n*-heptane), on the combustion characteristics within a typical aircraft engine. The combustion of conventional jet fuel (kerosene), biofuel (MB – surrogate fuel), and Fischer–Tropsch (FT) fuel has been investigated theoretically using computational fluid dynamics (CFD). For this fundamental study of the combustion process, the modern air-spray combustor (MAC) has been utilized. The CFD approach has previously been validated against the experimental measurements in the MAC for kerosene fuel [**4**, **5**]. Detailed oxidation mechanisms for kerosene and MB, recently developed by the authors [**6**], have been employed in the three-dimensional (3D) CFD solver using a mixture fraction/PDF approach. A detailed comparison of kerosene with alternative fuel performance has been made. Since fundamental information about the reaction kinetics is essential for a combustion model, these new reaction mechanisms facilitate the modelling of chemistry aspects required for an accurate combustion simulation. The synthetic fuel combustion scheme was represented by the *n*-heptane mechanism proposed by Seiser [**7**]. The available *n*-heptane mechanism is well understood and validated (National Institute of Standards and Technology) in comparison to other schemes such as *n*-decane and *n*-dodecane. Therefore, *n*-heptane has been used as a single component in this article to show an extreme of FT fuel. For modelling purposes, a reduced mechanism has been adopted.

2 ALTERNATIVE AVIATION FUELS – NEW CHALLENGES

Since their conception, aircraft gas turbines have utilized kerosene as a basic fuel because of its availability on a large scale and its robust stability properties combined with high energy content. Typical petroleum-based jet fuels such as Jet A and Jet A-1 (used in civil aviation) as well as JP-5 and JP-8 (utilized in military aircraft), have been developed extensively over a number of years. The composition of jet fuel, primarily based on wide ranging sizes of hydrocarbons (different molecular weight and carbon number), offers a relatively high volumetric and gravimetric energy [**8**, **9**].

The problems associated with using alternative fuels in aviation have attracted considerable attention recently and have become an internationally
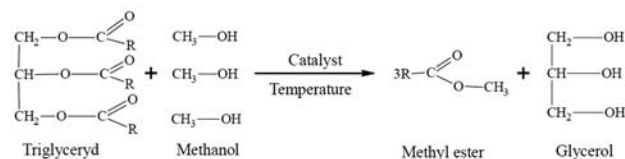
Fig. 1   Production of FAMEs – transesterification of triglycerides with alcohol

important topic for discussion. A number of studies have been published in which the performance of these alternative fuels has been examined [**4**, **6**, **10–13**]. The bio-jet fuels which are derived from sustainable sources can produce significant savings in carbon dioxide emissions, making them attractive for consideration. However, given that the aviation fuel specification requirements are very stringent, using a pure bio-jet fuel in aviation requires investigation, with direct replacement potentially requiring significant modifications to the engine design. The most common biodiesel developed and employed recently are the fatty acid methyl esters (FAMEs). Produced via a process of transesterification of oils and fats with methanol (Fig. 1), these esters have similar chemical and physical properties compared with conventional diesel fuel [**14**].

The esterification process brings changes in the structure of the vegetable oil molecules such as viscosity and saturation; thus, the properties of the final product (methyl ester) are different in comparison to jet fuel. A number of studies have shown that FAMEs can be used for aircraft transportation, in particular as a blended component. However, there are some properties (including freezing point, thermal stability, etc.) of biodiesels which are very poor compared to conventional jet fuel. Furthermore, the oxygen present in the biofuel molecule has an impact on the overall energy content. Consequently, the energy is lower (typical $LHV_{biofuel} = 36–39$ MJ/kg) when compared with conventional jet fuel (typical $LHV_{jet\,fuel} = 42$ MJ/kg). This is one of the major problems related to biofuels, since it results in the engine power profile being modified [**14**, **15**]. As such, with the current state of knowledge, it is still a technical challenge to use pure biofuel in a jet aircraft.

The synthetic fuel produced via the high-temperature FT method from coal, gas, or biomass is a further alternative, which has been studied for aviation purposes. The nature of the process is expressed by the exothermic reaction (1) listed below [**14**]

$$(2n + 1)H_2 + nCO \rightarrow C_nH_{(2n+2)} + nH_2O \qquad (1)$$

FT fuel has been implemented successfully in Johannesburg as a 50:50 blend by SASOL Limited (South Africa Synthetic Oil Liquid) and recently

100 per cent SASOL fuel has been approved for use in commercial aircraft. FT fuel is comparable in performance to conventional jet fuel and exhibits superior thermal stability. Experimental studies have shown that the FT product is almost entirely free of heteroatoms and aromatics, making it very attractive for use in both biodiesel and in jet applications. The major advantage of aromatic free fuels is that they are cleaner burning fuels with, generally, lower particulates remaining after combustion (no sulphur dioxide (SO_2) and sulphuric acid (H_2SO_4)) compared to those from the conventional jet fuel. However, this lack of aromatics results in FT fuel not meeting density requirements and also can cause problems due to issues relating to engine material compatibility [14]. This is a distinct disadvantage of synthetic fuels. Experiments show that the drawbacks can be reduced significantly when FT fuels are blended with jet fuel [13, 14].

3　COMBUSTION SYSTEM

A detailed description of the MAC engine has been provided in previous publications [4, 5]. Combustion simulations were carried out using the MAC shown in Fig. 2(a) to 2(c). For CFD simulation purposes, a single-burner port (1/22 of the combustion chamber) has been considered, assuming the rotational symmetry of the MAC. The structured mesh created for the MAC consists of 198 000 hexahedral and 3600 prismatic wedge elements. Fuel is injected as droplets (with a constant diameter of 20 μ and an initial temperature of 340 K) through a thin annulus (5.6 mm radius) located at the centre of the injector (Fig. 2(a) and 2(b)). The experimental operating pressure $P = 700$ kPa and corresponding air inlet temperature $T = 800$ K have been considered for the simulation. For the given conditions, the spray evaporates very quickly following it entering the combustor. Additional air is provided via the primary and dilution
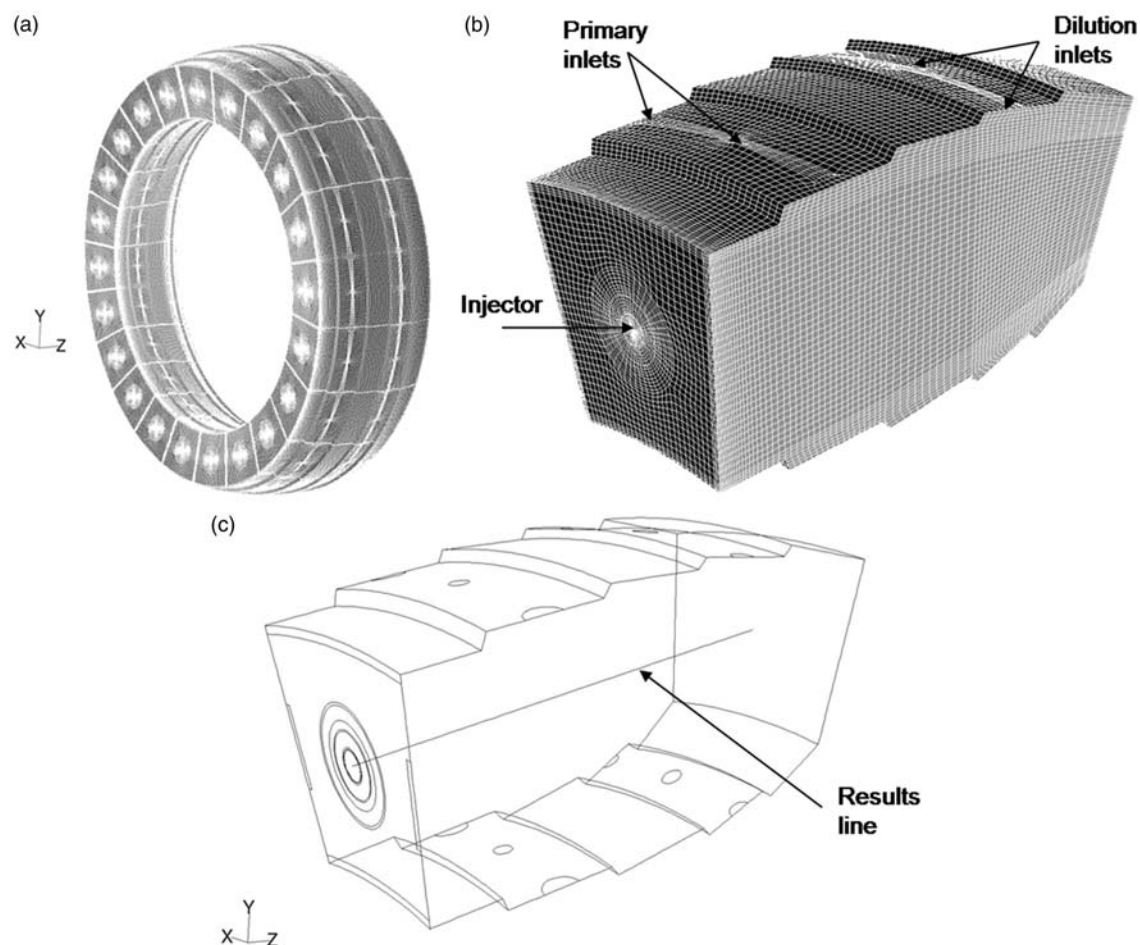
Fig. 2　The geometry of the combustor: (a) full annular geometry of the MAC with 22 burner ports; (b) meshed computational domain; and (c) geometry of the combustor section showing central line where the results can be compared
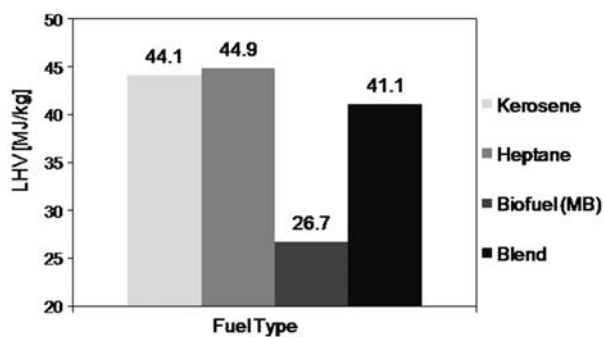
Fig. 3 Lower heating values are taken into account through normalization of input energy to the combustor by adjusting fuel mass flowrates accordingly

holes in the near-wall region of the inflow boundary conditions in order to complete the combustion process and cool the hot products leaving the combustor. The boundary conditions for both air and fuel inlets, as well as drop size and spray angles of the fuel for the model, have been calculated based on the experimental data taken from QinetiQ (formerly the UK's Defence Evaluation and Research Agency). In order to simplify and save computational time, it was decided not to include heat loss from the combustor in this model. In non-premixed (diffusion) flames, the impact of radiation losses is not typically significant due to the optical thickness. Therefore, a zero heat flux boundary condition (adiabatic case) is implemented for the combustor body. For the purposes of comparing CFD results, a line perpendicular to the injector, running along z-axis through the centre of the combustor, is marked in the Fig. 2(c).

Due to the differences in energy content of the alternative fuels compared with kerosene (Fig. 3), the mass flow has been recalculated to make the input energy per second equivalent for all fuels. This has been achieved by normalizing based on the mechanism for each fuel (taking the enthalpies into account). This approach is considered a more realistic approach for obtaining comparative engine performance, than simply comparing equivalent mass flowrates of fuel. Full research for a study of kerosene and biofuel combustion in the MAC based on equivalent fuel flowrates is presented in an earlier publication [4].

4 CFD MODELLING APPROACH

4.1 Turbulent combustion simulation

A range of different models have been applied during this investigation in order to solve the considered problem both efficiently and with high accuracy.

Based on steady-state Reynolds-averaged Navier–Stokes equations, the Reynolds stress model (RSM) has been applied to solve turbulent flow within the combustor. The RSM approach has been extensively examined for gas turbine combustion problems and is considered an accurate choice in the case of highly swirling flows. Consequently, using RSM is an efficient way to improve the simulation accuracy [16, 17].

The computational procedure includes the simulation of the full combustion process together with the injection of the fuel using the discrete phase model. With this approach, the computational domain is resolved for two phases, specifically the continuous phase and a Lagrangian discrete phase, where the main process transport equations are computed using Eulerian formulation and the calculation of the particle trajectories (discrete phase) is performed using a Lagrangian method. The Finite Volume Solver, Fluent 6.3 has been used in this study to numerically evaluate the sets of highly non-linear equations.

During the combustion process in an aero-engine, the products are not typically formed in a single chemical reaction; in fact, there tend to be hundreds of reactions to be included in the process. In view of the fact that the flow field is influenced by changes in temperature, density, and species concentration, there are additional equations to be solved. Additionally, if intermediate reactions are present, the solution procedure for the model will be more time consuming. When considering turbulent combustion phenomena, the problems are related to the complexity of the chemical kinetics and the strong non-linear connection between turbulence and chemistry. The turbulence–chemistry problem arises from the fact that generally the mixing process in combustion is slow in contrast with the chemical reaction rates. The major concern in this area is the capability of handling realistic finite-rate chemical kinetics with an accurate model.

Non-premixed flames can be used to describe general liquid combustion processes in gas turbines. The problem is simplified to the mixing and reaction of two opposing streams of fuel and oxidizer. The concept of the mixture fraction f is incorporated to express the degree of the scalar mixing between the fuel and oxidizer. The closure problem, in conjunction with a non-premixed model for the chemical source, has been solved by introducing the probability density function (PDF) of the fluctuating scalar variables. A statistical distribution of the mixture fraction f in the turbulent flow field is specified by a beta PDF function, which provides the information for the mean values of the fluctuating scalars,

i.e. temperature, density, and species mass fractions in the mixture fraction space [18, 19]. The shape of the assumed PDF is determined by the local mean mixture fraction and can be illustrated by the following mathematical formula (2). The PDF denoted by $p(f)$ represents the fraction of the time T that the fluid spends in the f state region.

$$p(f)\Delta f = \lim_{T \to \infty} \frac{1}{T} \sum_i \tau_i \qquad (2)$$

The laminar flamelet model (LFM) employed in this case in conjunction with the non-premixed model is based on the assumption that a turbulent diffusion flame appears as a steady, 1D laminar strained flame. This assumption holds in many applications for turbulent gas diffusion flames [18–20, 21]. A flamelet model gives a compromise between accuracy of results and simulation time for reacting flows and simultaneously incorporates the detailed chemical kinetics for the turbulent combustion simulations. In order to couple the impact of the flow field on the flame structure and shape, the flamelet library is created for two input parameters, the mixture fraction f and the so-called scalar dissipation rate χ. The relation between them is expressed by equation (3). Within the model, the scalar dissipation rate is considered as a parameter that incorporates the convection-diffusion effect in the mixture fraction space. The information enclosed in the flamelet library, in the form of look-up tables, incorporates species, density, and temperature profiles in the mixture fraction space required for further evaluation of the combustion characteristics and formation of pollutants.

$$\chi = 2D|\nabla f|^2 \qquad (3)$$

The principle of the flamelet generation is expressed by the following set of partial differential equations (4) and (5) listed below for the species mass fraction Y_i and temperature T for given scalar dissipation rates [18]

$$\rho \frac{\partial Y_i}{\partial t} = \frac{1}{2}\rho\chi \frac{\partial^2 Y_i}{\partial f^2} + S_i \qquad (4)$$

$$\rho \frac{\partial T}{\partial t} = \frac{1}{2}\rho\chi \frac{\partial^2 T}{\partial f^2} - \frac{1}{c_p}\sum_i H_i S_i$$

$$+ \frac{1}{2c_p}\rho\chi \left[\frac{\partial c_p}{\partial f} + \sum_i c_{p,i}\frac{\partial Y_i}{\partial f}\right]\frac{\partial T}{\partial f} \qquad (5)$$

The LFM approach incorporates the local finite chemistry effect, which results from turbulence influencing the thermochemical field. Different levels of the scalar dissipation incorporated into the flamelet calculations are primarily responsible for the variations in the structure of the flame.

For the multiple flamelet library generation, scalar dissipation rates of between 0.01 and 36.0 have been implemented.

NO$_x$ formation in turbulent reacting flows is a complex process that involves fluid dynamics, chemical kinetics, and mixing processes and requires hundreds of elementary reactions to be considered. In this article, the NO$_x$ is computed as a post-processor task since solving the pollutant species equations jointly with the combustion model is more complex and time consuming [22]. This is an efficient and reliable approach that involves solving additional transport equation (6) for the nitric oxide (NO) species concentration based on a calculated flow field (6). The thermal and prompt NO which have been employed in the computation are expressed in the reactions proposed by Zeldovich and Fenimore, respectively [23, 24]. The transport model included for NO$_x$ production is given as follows

$$\frac{\partial}{\partial t}(\rho Y_{NO}) + \nabla\cdot(\rho\vec{v}Y_{NO}) = \nabla\cdot(\rho D\nabla Y_{NO}) + S_{NO} \qquad (6)$$

5 THEORETICAL STUDY ON ALTERNATIVE AVIATION FUEL REACTION MECHANISM

Simulation of the combustion in a gas turbine requires a conceptual understanding of the process chemistry, as such an accurate reaction mechanism is essential. In this case, we require mechanisms for both the biofuel (MB) and heptane. In this study, a detailed chemical reaction mechanism AFRMv.2.0, recently developed and validated by Catalanotti *et al.* [6] which incorporates a number of different aviation fuels including both a conventional aviation fuel (kerosene) and biofuel (MB), has been implemented in the CFD simulations. The mechanism has previously been tested in several relevant areas including CHEMIKIN^{TM} – PSR and Premix simulations, in which robust results over a wide range of operating conditions were obtained (covering combustion temperature, pressure, and different equivalence ratios). The oxidation of *n*-heptane, represented by mechanism from Seiser *et al.* [7], has been applied to the calculations for predictions for the synthetic fuel. In this section, the performance of the mechanisms has been examined to predict the combustion chemistry within the aircraft engine with special concentration on the flame structure. Accordingly, the mechanism for each fuel along with a thermodynamic database has been applied to the 1D LFM to generate flamelet libraries (i.e. temperature and concentration of the species within the flame) each with a different scalar dissipation rate required for further simulations. The detailed kinetics

Table 1   Overview of the different fuel composition used for the flamelet calculations

Case	Component	Fuel composition – mole fraction (%)	Detailed reaction mechanism Number of species / Number of reactions
Kerosene	n-Decane – $C_{10}H_{22}$	89	203/1116
	Toluene – $C_6H_5CH_3$	11	
FT fuel (n-heptane)	n-Heptane – C_7H_{16}	100	166/824
Biofuel – MB (surrogate fuel)	Methyl butanoate – $C_5H_{10}O_2$	100	203/1116
Blend	Kerosene	80	203/1116
	Methyl butanoate	20	

of the considered fuel cases, as indicated in Table 1, have been incorporated into the calculations. This section provides the initial data related to the flame structure (prior to considering the specific geometry of the MAC), results of which are employed to the later CFD calculations within the model.

5.1 Comparison of chemical kinetics for alternative aviation fuels – OPPDIF

When undertaking this modelling approach, the first stage is to undertake opposed flow-diffusion flame (OPPDIF) calculations using the appropriate reaction mechanisms for each fuel. Figs 4 and 5 (a) to 5(d) outline the predictions for the temperature and mass fractions of CO_2, CO, O, and OH obtained from the OPPDIF calculations. In both Figs 4 and 5, the temperature and species mass fractions for each fuel are plotted against the mixture fraction, based on the two streams of fuel and oxidizer. An examination of the results of these calculations provides information on each fuel's combustion characteristics prior to solving the full CFD flow field for a particular combustor geometry. The dashed lines (f_1, f_2, f_3, f_4) denote the position of the stoichiometric mixture fraction for each fuel. It can be observed in Fig. 4 that the maximum flame temperature is comparable for pure kerosene and heptane which occurs at mixture fraction f_1, $f_2 \sim 0.07$. With regard to the blended fuel temperature profile, only a minor difference can be observed (f_3) compared to the kerosene. Consequently, it can be concluded that the oxygen from the methyl ester molecule has an effect on the overall temperature characteristic in the MB and blended fuel. The same trend can be observed for the mass fractions of major and minor species such as O and OH (Fig. 5(a) to 5(b)). There is good agreement between the kerosene and the blended case. This reinforces the conclusion that the combustion chemistry is not significantly impacted when using 20 per cent MB blended with 80 per cent kerosene fuel. With regard to MB, a considerable decrease in concentration of O and OH can be noticed. Additionally, the trend in Fig. 5(a) to 5(d)
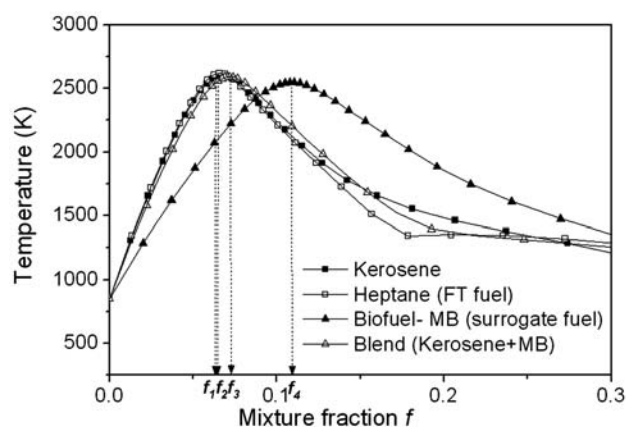
Fig. 4   OPPDIF calculations for the temperature

for O, OH, CO, CO_2, respectively, is similar to that in Fig. 4, where the maximum values predicted at richer mixture fractions are seen. Again, this can be attributed to the additional oxygen in the MB molecule. As such, a significant variation in the combustion chemistry is observed when kerosene is compared with 100 per cent MB. The peak of the flame temperature for MB (Fig. 4) is reached at a mixture fraction $f_4 \sim 0.12$ with a slightly lower peak temperature. From the combustion chemistry point of view, the deviations can be attributed to differences in the properties of the biofuel compared with conventional aviation fuel. Oxygen present in the methyl ester molecules indicates that there will be typically 10 per cent or greater oxygen content by mass in the biofuel. This will have an impact on the combustion chemistry in terms of the air-to-fuel ratio and emission levels. Additional oxygen included in the MB molecule takes part in combustion and appears to promote more complete combustion which partially explains variations in CO–CO_2 conversion.

The combustion kinetics of both kerosene and alternative fuels are determined by the molecular structure of the particular fuel components. The strength and energy of the molecular bonds in the different fuels are fundamentally responsible for the
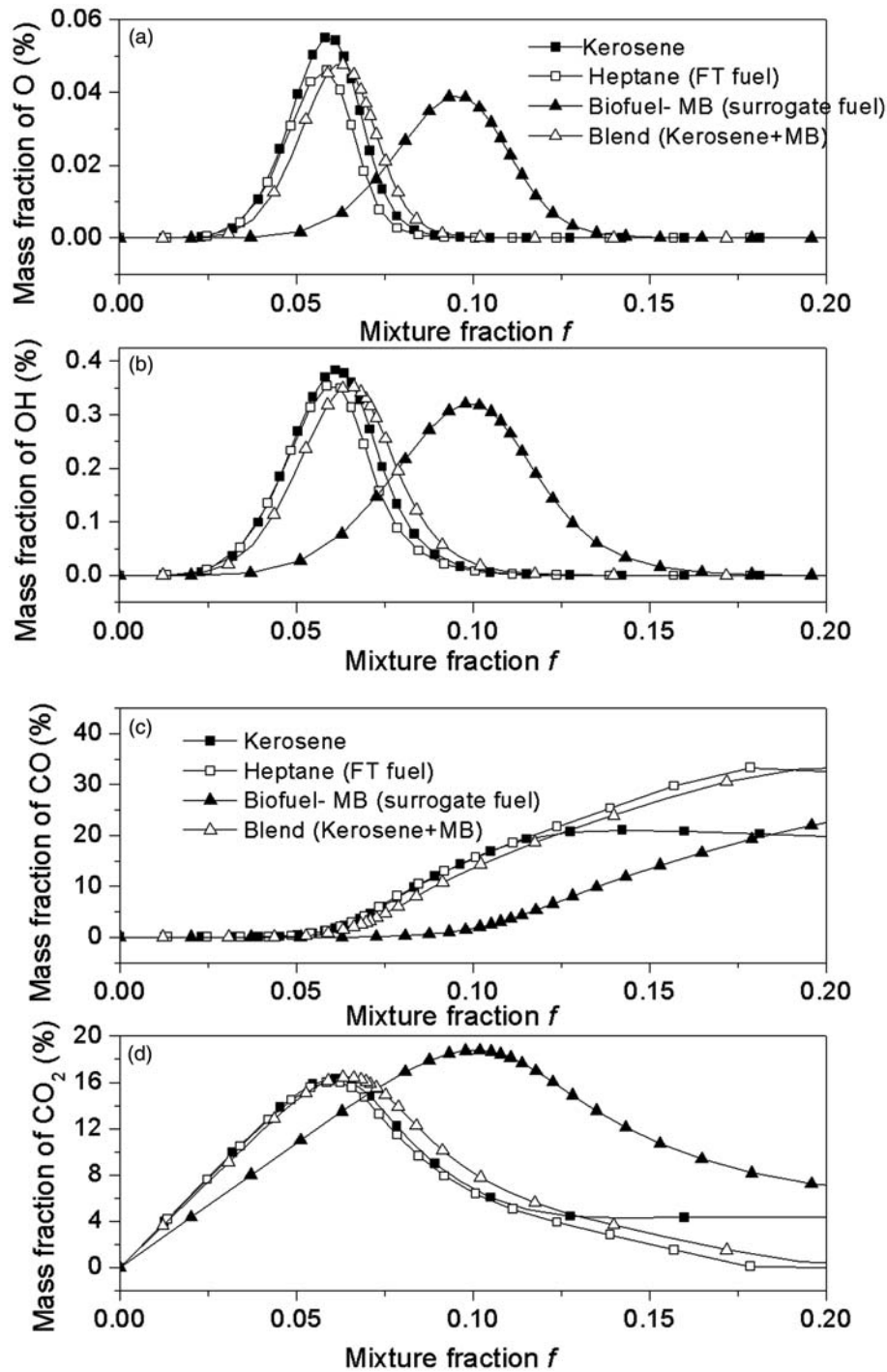
Fig. 5 OPPDIF calculations for: (a) mass fraction of O; (b) mass fraction of OH; (c) mass fraction of CO; (d) mass fraction of CO_2, respectively

path of the oxidation process. The presence of the ester grouping in FAMEs enhances the reactivity as it weakens the neighbouring C–C and C–H bonds next to the C=O group, due to resonance stabilization of the resulting radical that would be produced, thus enhancing the rate of decomposition or hydrogen abstraction in the FAME compared to normal alkanes [**6, 25, 26**].

In the case of heptane, it should be noted that, unlike kerosene, this fuel does not include aromatics and therefore there is the expected difference in the performance. The overall effect of aromatics is not fully clear in the combustion but this subject demands further investigation.

Finally, it has been identified that MB has a low combustion enthalpy, lower than that of kerosene
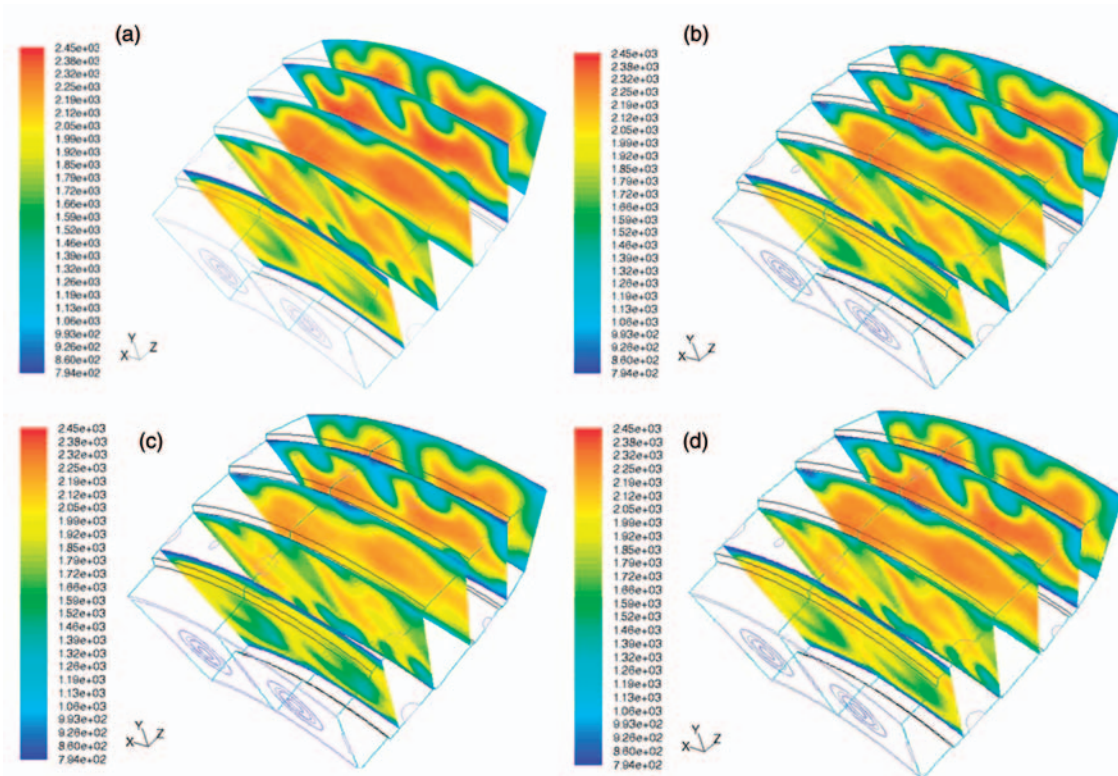
Fig. 6   Comparison of temperature contour plots for the fuels considered. From left, figures (a) to (d) represent, respectively, kerosene, n-heptane, MB, and blend

fuel due to the oxygen content of the molecules, which necessitates a larger fuel flow to the combustor in order to deliver the same amount of energy to that provided by kerosene. Further analysis of the combustion chemistry of the biofuel and synthetic fuel has been discussed by authors elsewhere [**17**, **18**, **20**].

6   DISCUSSION OF CFD PREDICTIONS

6.1   The performance of alternative fuels in the aero-engine combustion chamber

In this section, the predictions obtained from the full CFD simulation for each fuel's performance in the MAC are outlined. During this research, it has been observed that when modelling the turbulence, the accuracy of simulation performed using the RSM was significantly improved when compared with the standard k-ϵ model. As such, the results outlined in this article will focus on those produced using the RSM approach.

The results of numerical simulations are presented for the four fuels indicated in Table 1. Predictions for all fuels are based on equivalent energy content. In the first instance, models have been verified by reproducing the conditions and predictions for the combustion of kerosene in the MAC [**4**]. Following

previous successful validation of the modelling approach, predictions for the alternative fuel cases, where no current empirical data exist, are performed.

In Fig. 6 (a) to 6(d), simulation result data are displayed on planes parallel to the injector at the following positions relative to the burner: $Z = 0.038$ m, $Z = 0.068$ m, $Z = 0.106$ m, $Z = 0.14$ m, and $Z = 0.17$ m (where $Z = 0$ describes a plane that passes through the injector nozzle) are presented. These planes make useful comparison positions for validating the model predictions and observing the behaviour of the alternative fuels. In the predicted temperature contour plots, for kerosene, n-heptane, MB, and blend (Fig. 6(a) to 6(d)), an important observation is that the overall temperature distribution in the combustion chamber is comparable for all the considered fuels. When taking into account, the blend and n-heptane temperature profiles (Fig. 6(b) and 6(d), respectively), it can be observed that combustion chemistry is not significantly affected by the alternative fuel and there is no noticeable influence on the performance. However, it has been found that temperature for MB is slightly lower than that of the reference kerosene fuel (Fig. 6(a) and 6(c)). This discrepancy can be attributed to the oxygen in the methyl ester molecule impacting the combustion characteristics. Obviously, the physical properties of

the alternative fuel (lower heating value, density, etc.) can influence not only the efficiency of the overall system, but also the size of the tank and the weight of the aircraft. However, in the case, when the fuel flowrate is increased to take account of the reduced combustion enthalpy, the result for MB and blend can be observed to be much closer in character to that of kerosene, but with marginally reduced temperatures. The differences in predictions can be seen more clearly on the plots in Fig. 7(a) to 7(f), where the results of temperature and species mole fractions (O_2, CO, CO_2, H_2O, UHc), respectively, have been plotted for the range of fuels mixtures described in the Table 1 on the horizontal result line passing through the centre of the combustor (Fig. 2 (c)). As discussed earlier, the results outlined for kerosene have been validated against the experimental data. Therefore, those are considered as a base for the assessment of the alternative fuels performance.

Figure 7(a) refers to the temperature obtained within the combustion chamber. The results demonstrate that there is good agreement between all the

tested fuels. In Fig. 7(c) to 7(e), the predictions for CO, CO_2, and UHc mole fractions, respectively, have been plotted against the axial distance from the injector. It can be observed that for the intermediate temperature regions, where the concentration of OH appears to be lower, the level of CO and UHc is higher as a consequence of reduced conversion of CO to CO_2. Figure 7(e) illustrates a comparison of the water concentration for the indicated fuels. It can be observed that in the case of heptane, there is a low water concentration close to the injector. This is attributed to a deficit of oxygen in this region. It is also worth of note that the H/C ratio in C_7H_{16} is very high, which partially explains the reduction in the water mole fraction and which provides the peak in H_2 concentration.

Figure 8 shows the temperature data averaged at radial positions on the outlet. There are particularly meaningful data since they represent the predicted temperature that a turbine blade situated at the exit of combustor would experience. Any significant differences in temperature could have detrimental
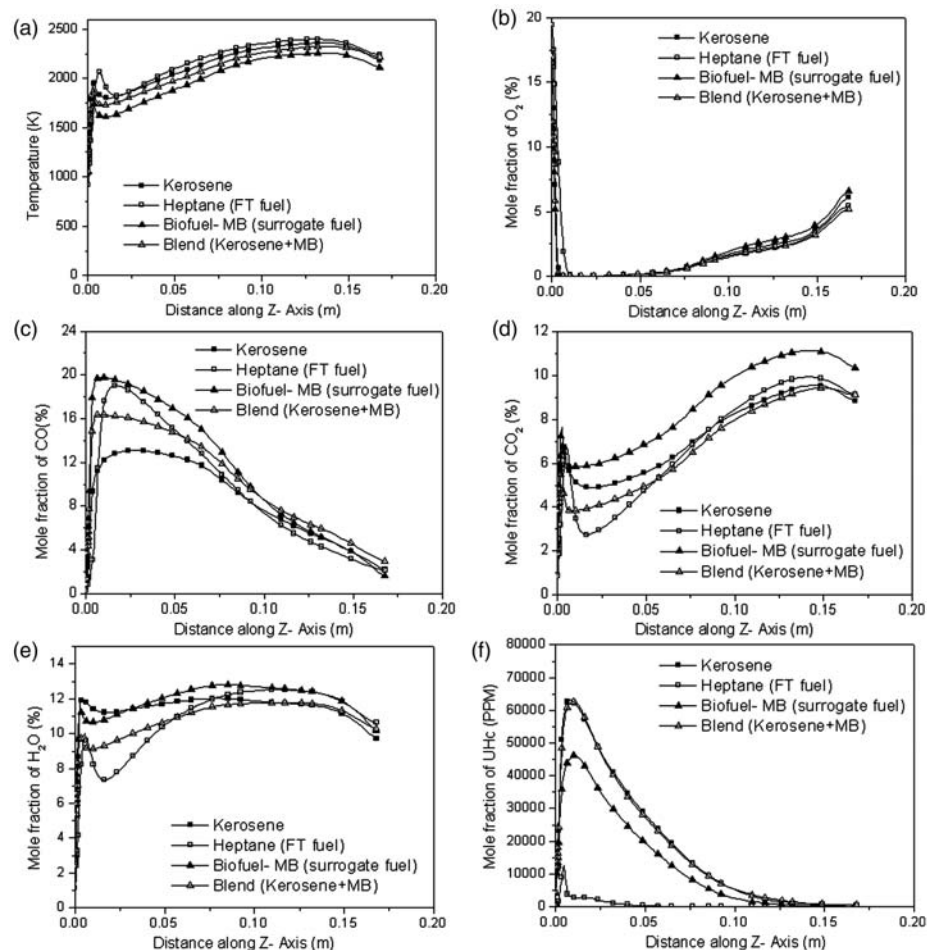
Fig. 7 Comparison of the CFD predictions for: (a) temperature; (b) O_2; (c) CO; (d) CO_2; (e) H_2O; and (f) UHc
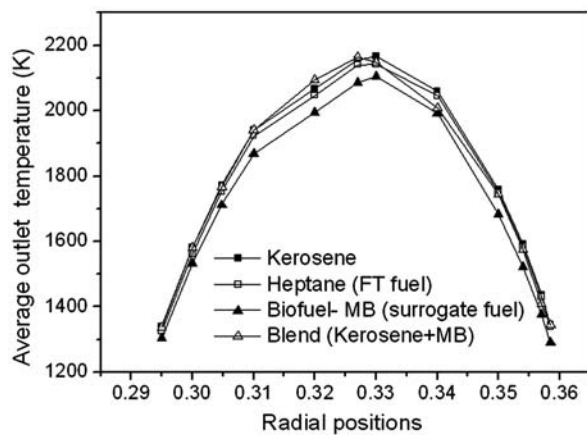
Fig. 8 CFD results for the average outlet temperature

Fig. 9 Comparison of theoretical CFD profiles of NO_x: (a) emission index of NO_x and (b) mole fraction of NO_x

consequences on the operating lifetime of the turbine blades which have been designed to be used with fuels that provide a distinctive temperature profile under typical operating conditions. These results do not indicate that this would be a significant problem in the case of the fuels investigated. However, the temperature profile for the MB is slightly lower in part due to the physical properties of the methyl ester.

6.2 Predictions for NO_x emissions

Investigating the impact on NO_x emissions and formation when using the alternative fuels was of prime importance in this study. For the purposes of this research, the NO_x production characteristics within the MAC combustor were computed with a partial equilibrium approach using the calculated temperature and species mixture fractions. The turbulence–chemistry interaction was modelled using a joint PDF approach.

The kinetics of thermal NO_x formation are governed by the Zeldovich mechanism where in accordance with the theory, NO_x can be formed from the atmospheric nitrogen at sufficiently high temperatures. The oxidation occurs mainly in the post-flame area, where the concentrations of major radicals O and OH are sufficient for the process to occur. Thermal method is the leading process for NO_x production at high temperatures (above 1800 K) in the gas turbine [**20**]. In contrast, prompt NO_x is supported by fuel-rich conditions since C_2H_2, as a precursor of the radical CH, is formed and accumulated under rich fuel combustion. As such, it supplies only around 10 per cent of total NO_x formed in the engine [**20**, **22**, **27**].

The predicted thermal and prompt NO_x profiles along the centre of the combustor are shown on

Fig. 9(a) to 9(b). In Fig. 9 (a), the mole fraction of NO_x is given for each fuel in parts per million, whereas in Fig. 9 (b) the exhaust NO_x emissions are evaluated using the emission index, (NO_x), defined as the grams of NO_x per kilogram of fuel burned. For all cases, the predicted values indicate the correct trend of increasing NO_x concentration towards the combustor outlet. The NO_x concentrations for MB and blend were found to be lower than for conventional kerosene fuel. The differences in the predicted NO_x concentration between kerosene (baseline) and the alternative fuels can be attributed to disparity in the flame location and the O and OH concentrations which are important in NO_x formation processes. Reduced temperatures in the case of MB and blend result in decreases in NO_x. It should be noted that the NO_x emissions are strongly temperature-dependent phenomena and, therefore, the lower level of NO_x emissions may be primarily due to the lower temperature on the outlet of the combustor.

7 CONCLUDING REMARKS

In this article, the properties of two alternative aviation fuels, synthetic kerosene (*n*-heptane) and bio-aviation fuel (MB), have been compared against kerosene for their combustion performance in a MAC. This has been achieved using the recently developed detailed reaction mechanisms, AFRMv2.0 and *n*-heptane, coupled to a CFD simulation approach. The CFD predictions for kerosene were previously validated against experimental data. The objective of this study was to evaluate the effect of using alternative fuel on the combustion characteristics.

The following conclusions can be drawn from this study:

1. The impact of using the blended fuel has been shown to be very similar in combustion performance to that of the 100 per cent kerosene. A combustor can perform satisfactorily using blended fuel (MB and kerosene). Based on the performance results, it has been identified that 20 per cent methyl butanoate blend is an acceptable concentration for biofuel.
2. The use of heptane (synthetic fuel) appears to provide comparable results to that of kerosene when considering overall performance. However, further research is required to understand the consequences of using synthetic fuels with respect to a range of issues including that of their low aromatics content.
3. The differences in properties between biofuel (MB) and jet fuel (viscosity, density, and energy content) are considered to be responsible for a variation in the combustion performance. Based on the theoretical investigations, in this article, it can be concluded that biofuel (MB) cannot be directly adopted as an alternative fuel for existing engines without modifications being required to the system. When using the 100 per cent MB, with increased fuel flowrates to normalize the energy content, the combustion characteristics are much more closely aligned to those of kerosene. However, under these conditions, the additional amount of fuel transferred to the combustion chamber (and associated design requirements for this) will impact on the overall engine and fuel system performance. This aspect of the work requires further experimental study in order to provide a detailed understanding of the issues and as a means to confirm the accuracy of the predicted results.

ACKNOWLEDGEMENTS

REFERENCES

1 Federal Aviation Administration. Aviation and the environment - managing the challenge of growth, NASA Fundamental Aeronautics Meeting, FAA Office of Environment and Energy, Washington, DC, 30 October 2007.
2 **Penner, J. E., Lister, D. H., Griggs, D. J., Dokken, D. J.,** and **Mcfarland, M.** *Summary for policymakers: aviation and the global atmosphere, A special report of IPCC Working Groups I and III: Published for the Intergovernmental Panel Climate Change*, 1999 (Cambridge University Press, New York).
3 **The European Commission.** Biofuels in the European Union. A vision for 2030 and beyond, Brussels, 8 June 2006.
4 **Uryga-Bugajska, I., Pourkashanian, M., Borman, D., Catalanotti, E., Ma, L.,** and **Wilson, C. W.** Assessment of the performance of alternative aviation fuel in a modern air-spray combustor (MAC). In Proceedings of ASME IMECE 2008, Boston, MA, 2–6 November 2008.
5 **Kyne, A. G., Pourkashanian, M., Wilson, C. W.,** and **Williams, A.** Validation of a flamelet approach to modelling 3-D turbulent combustion within an air-spray combustor. In Proceedings of ASME Turbo Expo: Land, Sea and Air 2002, Amsterdam, The Netherlands, 3–6 June 2002.
6 **Catalanotti, E., Hughes, K. J., Pourkashanian, M., Uryga-Bugajska, I.,** and **Williams, A.** Development of a high temperature oxidation mechanism for bio-aviation fuels. In Proceedings of ASME IMECE 2008, Boston, MA, 2–6 November 2008.
7 **Seiser, R., Pitsch, H., Seshadri, K., Pitz, W. J.,** and **Curran, H. J.** Extinction and autoignition of n-Heptane in counterflow configuration. *Proc. Combust. Inst.*, 2000, **28**, 2029–2037.
8 **Heminghaus, G., Boval, T., Bosley, C., Organ, R., Lind, J., Brouette, R., Thomson, T., Lynch, J.,** and **Jones, J.** *Aviation fuels technical review*, 2006 (Chevron Products Company Inc, San Ramon, CA).
9 **Maurice, L. Q., Lander, H., Edwards, T.,** and **Harrison III, W. E.** Advanced aviation fuels: a look ahead via a historical perspective. *Fuel*, 2001, **80**, 747–756.
10 **Dagaut, P.** and **Gail, S.** Kinetics of gas turbine liquid fuels combustion: Jet-A1 and bio-kerosene. In Proceedings of GT2007, Montreal, Canada, 14–17 May 2007.
11 **Gail, S., Thomson, M. J., Sarathy, S. M., Syed, S. A., Dagaut, P., Dievart, P., Marchese, A. J.,** and **Dryer, F. L.** A wide-ranging kinetic modelling study of methyl butanoate combustion. *Proc. Combust. Inst.*, 2007, **31**, 305–311.
12 **Metcalfe, W. K., Dooley, S., Curran, H. J., Simmie, J. M., El-Nahas, A. M.,** and **Navarro, M. V.** Experimental and modelling study of $C_5H_{10}O_2$ethyl and methyl esters. *J. Phys. Chem. A*, 2007, **111**, 4001–4014.
13 **Moses, C. A.** and **Roets, P. N. J.** Properties, characteristics and combustion performance of SASOL fully synthetic jet fuel. In Proceedings of GT2008, Berlin, Germany, 9–13 June 2008.
14 **Daggett, D. L., Hendricks, R. C., Walther, R.,** and **Corporan, E.** Alternate fuel for use in commercial aircraft, 2007, The Boeing Company, Seattle, WA.

15 Ebbinghaus, A. and **Wiesen, P.** Aircraft fuels and their effect upon engine emissions. *Air Space Eur.*, 2001, **3**, 24–50.

16 Bilger, R. W. Future progress in turbulent combustion and research. *Prog. Energy Combust. Sci.*, 2000, **26**, 367–380.

17 Leschinzer, M. A. Modelling engineering flows with Reynolds stress turbulence closure. *J. Wind Eng. Ind. Aerodyn.*, 1990, **35**, 21–47.

18 Patterson, P. M., Kyne, A. G., Pourkashanian, M., Williams, A., and **Wilson, C. W.** Combustion of kerosene in counter-flow diffusion flames. *AIAA J. Propul. Power*, 2001, **17**(2), 453–460.

19 Peters, N. Laminar diffusion flamelet models in non premixed combustion. *Prog. Energy Combust. Sci.*, 1984, **10**, 319.

20 Warnatz, J., Maas, U., and **Dibble, R. W.** *Combustion: physical and chemical fundamentals, modelling and simulation, experiments, pollutant formation*, 2001 (Springer, Berlin).

21 Riesmeier, E., Honnet, S., and **Peters, N.** Flamelet modelling of pollutant formation in gas turbine combustion chamber using detailed chemistry for a kerosene model fuel. *J. Eng. Gas Turbines Power (ASME)*, 2004, **126**, 899–905.

22 Hill, S. C. and **Smoot, L. D.** Modelling of nitrogen oxides formation and destruction in combustion systems. *Prog. Energy Combust. Sci.*, 2000, **26**, 417–458.

23 Heyl, A. and **Bockhorn, H.** Flamelet modelling of NO Formation in laminar and turbulent diffusion flames. *Chemosphere*, 2001, **42**, 449–462.

24 Miller, J. A. and **Bowman, C. T.** Mechanism and modelling of nitrogen chemistry in combustion. *Prog. Energy Combust. Sci.*, 1989, **115**, 287–338.

25 Gail, S., Thomson, M. J., Sarathy, S. M., Syed, S. A., Dagaut, P., Dievart, P., Marchese, A. J., and **Dryer, F. L.** A wide-ranging modelling study on methyl butanoate combustion. *Proc. Combust. Inst.*, 2007, **31**, 305–311.

26 Dooley, S., Curran, H. J., and **Simmie, J. M.** Autoignition measurements and a validated kinetic model for the biodiesel surrogate, methyl butanoate. *Combust. Flame*, 2008, **153**, 2–32.

27 Tsague, L., Tsogo, J., and **Tatietse, T. T.** Prediction of the production of nitrogen oxide (NOx) in turbojet engines. *Atmos. Environ.*, 2006, **40**, 5727–5733.

APPENDIX

Notation

c_p	mixture-averaged specific heat (J/kg K)
$C_{p,i}$	Specific heat of species i (J/kg K)
D	diffusion coefficient (m^2/s)
f	mixture fraction (dimensionless)
f	stoichiometric mixture fraction
$EI_{(NO_x)}$	emission index of NO_x (g/kg)
H_i	specific enthalpy of species i (J/kg)
LHV	lower calorific value (MJ/kg)
p	probability density function
P	pressure (kPa)
S	source term
S_i	reaction rate of species i (units vary)
t	time (s)
T	temperature (K)
$\vec{v}$	overall velocity vector (m/s)
Y_i	Mass fraction of species i (dimensionless)
Δ	Change in a variable
ρ	Density (kg/m^3)
τ_i	time scale (s)
T	time scale (s)
χ	Scalar dissipation rate (s^{-1})

Subscripts

Z	axial direction
$1,\ldots 4$	fuel stoichiometric mixture fraction state points